

***RHIC Optics Measurement with Different Working
Point***

R. Calaga, M. Bai, S. Peggs, T. Roser, T. Satogata

*Presented at the 9th European Particle Accelerator Conference
Lucerne, Switzerland
July 5-9, 2004*

July 2004

Collider-Accelerator Department

Brookhaven National Laboratory

P.O. Box 5000

Upton, NY 11973-5000

www.bnl.gov

Managed by

Brookhaven Science Associates, LLC

for the United States Department of Energy under

Contract No. DE-AC02-98CH10886

DISCLAIMER

This report was prepared as an account of work sponsored by an agency of the United States Government. Neither the United States Government nor any agency thereof, nor any of their employees, nor any of their contractors, subcontractors, or their employees, makes any warranty, express or implied, or assumes any legal liability or responsibility for the accuracy, completeness, or any third party's use or the results of such use of any information, apparatus, product, or process disclosed, or represents that its use would not infringe privately owned rights. Reference herein to any specific commercial product, process, or service by trade name, trademark, manufacturer, or otherwise, does not necessarily constitute or imply its endorsement, recommendation, or favoring by the United States Government or any agency thereof or its contractors or subcontractors. The views and opinions of authors expressed herein do not necessarily state or reflect those of the United States Government or any agency thereof.

FOR UNCLASSIFIED, UNLIMITED STI PRODUCTS

Available electronically at:

OSTI:

<http://www.osti.gov/bridge>

Available for a processing fee to U.S. Department of Energy and its contractors, in paper from:

U.S. Department of Energy
Office of Scientific and Technical Information
P.O. Box 62
Oak Ridge, TN 37831
Phone: (865) 576-8401
Facsimile: (865) 576-5728
E-mail: reports@adonis.osti.gov

National Technical Information Service (NTIS):

Available for sale to the public from:

U.S. Department of Commerce
National Technical Information Service
5285 Port Royal Road
Springfield, VA 22131
Phone: (800) 553-6847
Facsimile: (703) 605-6900
Online ordering: <http://www.ntis.gov/ordering.htm>



Printed on recycled paper

Submitted to EPAC'04, Lucerne, Switzerland, July 5-9, 2004

RHIC Optics Measurement with Different Working Point*R. Calaga, M. Bai, S. Peggs, T. Roser, T. Satogata
BNL, Upton, NY 11973, USA**Abstract**

Working point scans at RHIC were performed during 2004 to determine the effect on lifetime and luminosity. Linear optics were measured for different working point tunes by exciting coherent oscillations with the aid of RHIC AC dipoles. Two methods are currently used to measure the beta functions and phases advances: a conventional fitting technique, and an alternate method based on singular value decomposition (SVD). This paper focuses on the effect of working point on the measurement of linear optics using a SVD based technique. The use of a 3-bump beta wave algorithm to identify quadrupole error sources is also presented.

INTRODUCTION

A working point (tune) scan was performed at RHIC as a part of beam experiments to investigate the effect of lifetime and luminosity in run 2004 with Au-Au collisions [1]. For the PP 2004 run, tunes $(Q) \sim 0.72$ were chosen to be the new working point as a result of the previous study to improve polarization, luminosity and lifetime. RHIC is equipped with two AC dipoles capable of adiabatically exciting coherent betatron oscillations in both transverse planes, when driven close to the betatron tune, given by

$$x(s) = \frac{B_d L}{4\pi B \rho \delta} \sqrt{\beta(s)\beta_0} \sin(2\pi Q_x t + \psi(s)) \quad (1)$$

where $B_d L$ is the integrated AC dipole strength, $B\rho$ is the magnetic rigidity, $\beta(s)$ and β_0 are beta functions at the s and at the AC dipole respectively, δ is the tune separation between drive and intrinsic tune Q_x and $\psi(s)$ is the phase advance at location s . Turn-by-turn data acquired using beam position monitors (BPMs) is routinely used to compute linear optics at RHIC using coherent oscillations driven by the AC dipole. Linear optics were measured during these scans to understand the effects of tune on optics. Two techniques are currently used to determine Twiss parameters (phase advances, beta functions). We focus on the SVD based technique to measure linear optics crucial for machine operation and development of an accurate model.

SVD Technique

A model independent technique using SVD has been recently demonstrated to be accurate and robust [2, 3] in measuring linear optics using BPM data. SVD decomposition of a BPM data matrix consisting of turn-by-turn data (with closed orbit removed) from many BPMs is useful in the

determination of dominant physical patterns of the beam motion. In the presence of coherent betatron oscillations with small coupling, SVD decomposes the BPM matrix in two leading spatio-temporal eigenmodes representing the betatron modes. This decomposition can be analytically derived by solving the secular equation of the variance-covariance matrix $C_B = B^T B$. The normalized temporal (u_{\pm}) and spatial (v_{\pm}) vectors are given by [3].

$$v_{+} = \frac{1}{\sqrt{\lambda_{+}}} \left[\sqrt{\langle J \rangle} \beta_m \cos(\phi_0 + \psi_m) \right] \quad (2)$$

$$v_{-} = \frac{1}{\sqrt{\lambda_{-}}} \left[\sqrt{\langle J \rangle} \beta_m \sin(\phi_0 + \psi_m) \right] \quad (3)$$

$$u_{+} = \sqrt{\frac{2J_t}{T\langle J \rangle}} \cos(\phi_t - \phi_0) \quad (4)$$

$$u_{-} = -\sqrt{\frac{2J_t}{T\langle J \rangle}} \sin(\phi_t - \phi_0) \quad (5)$$

where J_t and ϕ_t are the action angle variable, β_m and ψ_m are the beta function and phase advance at the m^{th} BPM, λ_{\pm} are the square roots of the singular values σ_{\pm} , and t is the number of turns. The Twiss functions can be derived from the spatial vectors given by

$$\psi = \tan^{-1} \left(\frac{\sigma_{-} v_{-}}{\sigma_{+} v_{+}} \right) \quad (6)$$

$$\beta = \langle J \rangle^{-1} (\lambda_{+} v_{+}^2 + \lambda_{-} v_{-}^2) \quad (7)$$

Only the scaling factor $\langle J \rangle$ has to be determined from the model. The error bounds for the Twiss parameters are given by

$$\sigma_{\psi} \approx \frac{1}{\sqrt{T}} \frac{\sigma_{\tau}}{\sigma_s}, \quad \sigma_{\frac{\Delta\beta}{\beta}} \approx 2\sigma_{\psi} \quad (8)$$

MEASUREMENTS

Limitations in measuring Twiss functions are mainly related to the quality and availability of reliable BPM data. Performance of RHIC BPMs has been studied in detail and it was found that significant number of BPMs exhibit failures related to radiation, electronics and low level software issues [4]. These BPMs are removed before the Twiss parameters are calculated. It was also found that a few BPMs show turn mismatch due to timing problems in the electronics which are corrected in this analysis. Figs. 1 and 2 show a comparison between model and measured Twiss functions for Au-Au injection ($\gamma = 10.52$) and PP injection ($\gamma = 25.94$). The rms of the phase advance difference, $(\psi_m^{\text{model}} - \psi_m^{\text{measured}})$ and the rms of percent difference in β function, $(\beta_m^{\text{model}} - \beta_m^{\text{meas}})/\beta_m^{\text{model}}$ were calculated to understand the sensitivity of optics measurements to the

* This work was performed under the auspices of the US Department of Energy contract # DE-AC02-98CH10886

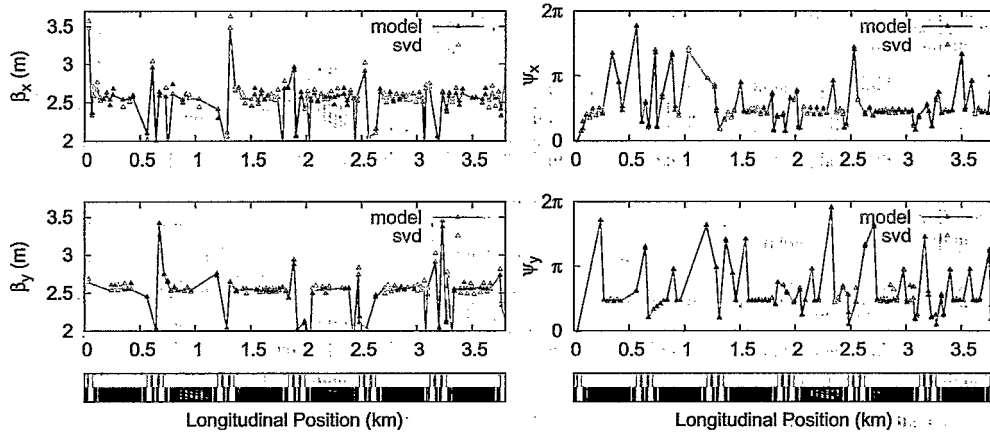


Figure 1: Phase advance and beta function for Au-Au injection optics using AC dipole.

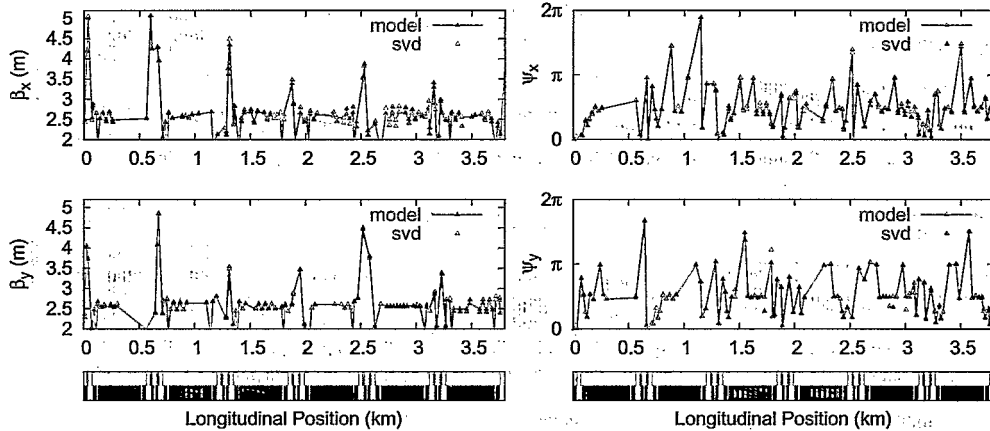


Figure 2: Phase advance and beta function for PP Injection optics using AC dipole.

working point and β^* . Some measurements show large deviation from the model mainly due to BPM failures. Data files with very large deviation are not included in this analysis. The measurement for Yellow and Blue ring were not separated because we assume that the instrumentation in both rings are similar.

Tables 1 and 2 show a detailed list of rms differences for the different working points at injection and store. One has to note that the model tunes are not exactly matched to measured tunes [5]. Fig. 3 shows a plot of average values and their standard deviations of $(\Delta\beta/\beta)^{rms}$ and $\Delta\psi^{rms}$ only for Au-Au and PP injection and store conditions. The other working points are not plotted because of large systematic errors. It is clear from Fig. 3 that deviation from the mean values are large mainly due to systematic errors. A number of systematic measurements and improvements in BPM reliability will reduce these deviations significantly. One can notice that the rms phase advance difference for $Q \sim 0.2$ region appears to be slightly better than $Q \sim 0.7$ region. One can also notice that for $Q \sim 0.2$ region, the $(\Delta\beta/\beta)^{rms}$ is smaller for injection optics ($\beta^* = 10m$) than store optics ($\beta^* = 1m$) as expected. However, the region near $Q \sim 0.7$ shows contrary results which needs

to be verified. A large number of statistics are needed to arrive at a definitive conclusion.

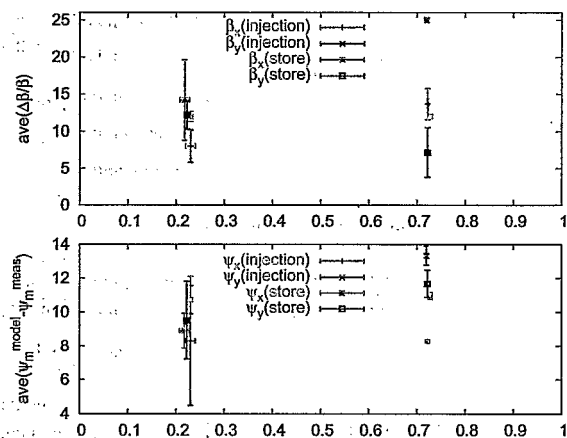


Figure 3: $(\psi_{model} - \psi_{meas})^{rms}$ and $(\Delta\beta/\beta)^{rms}$ for working points Au-Au and PP injection and store.

Table 1: Working point Optics at Injection($\gamma_{Au} = 10.52$, $\gamma_{pp} = 25.94$). β^* @ 6 IPs (10,10,10,10,10,10) [m]: NE - Not Estimated due to excitation of AC dipole in only one plane or large systematic errors.

Ring	Q_x	Q_y	$\Delta\psi_x^{rms}$	$\frac{\Delta\beta_x}{\beta_x}^{rms}$	$\Delta\psi_y^{rms}$	$\frac{\Delta\beta_y}{\beta_y}^{rms}$
RHIC Au-Au						
B	0.237	0.222	11.9	8 %	NE	NE
B	0.237	0.222	11.31	7 %	9.4	12 %
Y	0.21	0.22	10.9	NE	10.4	14 %
B	0.238	0.20	6.7	10 %	8.27	8 %
B	0.238	0.20	5.9	11 %	8.6	18 %
Y	0.219	0.232	2.5	5 %	8.6	17 %
B	0.238	0.224	11.46	7 %	10.1	23 %
B	0.238	0.224	NE	NE	7.5	8 %
RHIC PP						
Y	0.723	0.720	8.19	12 %	14	25 %
Y	0.723	0.720	8.3	13 %	13	NE
Y	0.723	0.720	8.36	16 %	13	NE
RHIC Design (Au-Au)						
Y	0.168	0.182	16.1	48 %	9.57	NE
Y	0.168	0.182	4.79	33 %	NE	NE
Y	0.201	0.187	2.13	19 %	9.8	32 %
Y	0.201	0.187	15.4	39 %	6.5	12 %
ISR (Au-Au)						
B	0.1025	0.11	10.9	13 %	22.3	52 %
B	0.1025	0.11	NE	NE	22.4	31 %
B	0.1025	0.11	NE	NE	15	8 %
SPS (Au-Au)						
B	0.705	0.695	13.3	25 %	20.07	39 %
B	0.705	0.695	17.0	23 %	17.7	36 %
B	0.705	0.695	NE	NE	14.5	9 %
B	0.705	0.695	NE	NE	12.3	9 %

Table 2: Working Point Optics at Store.

Ring	Q_x	Q_y	$\Delta\psi_x^{rms}$	$\frac{\Delta\beta_x}{\beta_x}^{rms}$	$\Delta\psi_y^{rms}$	$\frac{\Delta\beta_y}{\beta_y}^{rms}$
RHIC Au-Au						
$\beta^*(3,5,1,1,3,5)$ [m], $\gamma = 107.76$						
B	0.231	0.223	10.3	12 %	8.0	11 %
B	0.231	0.223	10.7	13 %	7.0	11 %
B	0.231	0.223	10.0	13 %	11.2	12 %
B	0.231	0.223	11.9	12 %	11.9	15 %
RHIC PP						
$\beta^*(3,10,2,2,3,10)$ [m], $\gamma = 106.58$						
Y	0.728	0.722	10.8	12 %	10.7	11 %
Y	0.728	0.722	10.9	12 %	11.93	6 %
Y	0.728	0.722	11.19	12 %	12.36	5 %

ERROR SOURCE IDENTIFICATION

The close analogy between trajectory and beta wave perturbations indicates a close connection between the problems of closed orbit correction and quadrupole error source identification. A thin horizontal focusing error of Δq [m⁻¹] causes a horizontal perturbation wave that propagates downstream to first order in Δq like

$$\frac{\Delta\beta}{\beta} \approx -\Delta q \beta_0 \sin(2(\phi - \phi_0)) \quad (9)$$

where β_0 is the design horizontal beta function at the quadrupole error source. Just as 3-dipole correctors can be powered to create a closed orbit “three-bump”, so also can 3 quadrupoles create a local beta-bump – if their strengths (Left, Right, and Center) are

$$\Delta q_L = -\frac{\Delta\beta_C}{\beta_C} \frac{1}{\beta_L} \frac{1}{\sin(2\phi_{CL})}$$

$$\Delta q_C = +\frac{\Delta\beta_C}{\beta_C} \frac{1}{\beta_C} \frac{\sin(2\phi_{RL})}{\sin(2\phi_{RC}) \sin(2\phi_{CL})} \quad (10)$$

$$\Delta q_R = -\frac{\Delta\beta_C}{\beta_C} \frac{1}{\beta_R} \frac{1}{\sin(2\phi_{RC})}$$

and where, for example,

$$\Delta\phi_{CL} = \phi_{Center} - \phi_{Left} \quad (11)$$

This beta-bump is not closed in the other (vertical) plane. The “sliding 3-bump” algorithm is often used in closed orbit correction applications, taking as input a vector of closed orbit displacements measured at many beam position monitors, and generating as output a vector of suggested dipole corrector adjustments. The algorithm is readily modified to take a measured $\Delta\beta/\beta$ vector as input, generating a suggested quadrupole correction vector (with elements at every lattice quadrupole) as output. It is often more practical to interpret this output vector as a set of quadrupole error sources, especially if the quadrupoles are powered as families (as in RHIC). If independent horizontal and vertical optics error measurements are available, then both measurements should identify the same quadrupole error sources. An off-line code `qlawb` is under testing, to automate source identification in this fashion.

SUMMARY

The measurement of linear optics using AC dipole was demonstrated reliably in Run 2003-4. Optics were measured for different working point tunes and a detailed comparison for each working point was done to understand the effect of tune. Although the region near $Q \sim 0.2$ shows slightly better results than the region near $Q \sim 0.7$, no significant difference was found between the working points. The effect of β^* is consistent for data near $Q \sim 0.2$ region. The region near $Q \sim 0.7$ needs to be revisited and more systematic studies will help develop a more accurate model.

ACKNOWLEDGEMENTS

We would like to thank all the RHIC operations group for helping during the experiments.

REFERENCES

- [1] R. Tomás et. al., Quest for a new working point in RHIC, these proceedings.
- [2] J. Irwin, C.X. Wang, Y. Yan, et.al., Phys. Rev. Lett. 82(8), 1684(1999).
- [3] C.X. Wang, et.al., Phys. Rev. ST Accel. Beams 6, 104001(2003).
- [4] R. Calaga, R. Tomás, Phys. Rev. ST Accel. Beams 7, 042801(2004).
- [5] J. van Zeijts, Transverse Optics Improvements for RHIC Run 4, this proceedings.